

Possible influence of neutron shell closure ($N_c = 126$) on fission anisotropies for $^{19}\text{F} + ^{194,198}\text{Pt}$ systems

K. Mahata, S. Kailas, A. Shrivastava, A. Chatterjee, P. Singh, and S. Santra
Nuclear Physics Division, Bhabha Atomic Research Centre, Mumbai 400 085, India

B. S. Tomar

Radiochemistry Division, Bhabha Atomic Research Centre, Mumbai 400 085, India

(Received 16 July 2001; published 27 February 2002)

Fission fragment angular distributions have been measured for $^{19}\text{F} + ^{194,198}\text{Pt}$ systems in the laboratory energy range from 88 to 104 MeV and the fission fragment angular anisotropy data have been compared with the statistical saddle-point model calculations. The anisotropy data for $^{19}\text{F} + ^{198}\text{Pt}$ (^{217}Fr with compound nucleus neutron number $N_c = 130$) are in good accord with the calculations over the entire range of bombarding energies except at the highest energy point. However, the data for $^{19}\text{F} + ^{194}\text{Pt}$ (^{213}Fr with $N_c = 126$) though consistent on the average with the calculations, show noticeable deviation at a few energies.

DOI: 10.1103/PhysRevC.65.034613

PACS number(s): 25.70.Jj

I. INTRODUCTION

Observation of anomalous fission fragment anisotropies in $^{12}\text{C} + ^{198}\text{Pt}$ system (^{210}Po , with compound nucleus neutron number $N_c = 126$) and normal anisotropies in $^{12}\text{C} + ^{194}\text{Pt}$ system (^{206}Po , $N_c = 122$) has been reported by Shrivastava *et al.* [1]. It has been observed that the measured anisotropies for $^{12}\text{C} + ^{198}\text{Pt}$ system are significantly larger than those of the statistical saddle-point model (SSPM) [2] predictions and the disagreement increases as the excitation energy (E_X) of the compound nucleus decreases. However, the anisotropy data for $^{12}\text{C} + ^{194}\text{Pt}$ system do not show any deviation with respect to theory over the entire energy range. To understand this feature, the authors had speculated that shell effects in the potential energy surface were perhaps influencing the fission anisotropies. This result also implied that shell effects are still not completely washed out at the saddle point even at high excitation energies, for a compound nucleus with $N_c = 126$. In fact, almost two decades back Vigdor *et al.* [3] had suggested the need for systematic fission fragment angular distribution measurements, as multichance high spin fission could enhance the sensitivity to shell corrections. Recently, Djerroud *et al.* [4] from systematic fusion studies related to $A \sim 190$, have indicated the possible importance of shell corrections, in particular, at the saddle point. It is of interest to extend the investigation to some more systems to verify the correlation between $N_c = 126$ of the compound nucleus and observation of anomalous anisotropies reported earlier [1]. In particular, this will help in ruling out any effect associated with target mass number used in the previous measurement.

With this motivation, fission fragment angular distributions have been measured for $^{19}\text{F} + ^{194,198}\text{Pt}$ systems. It may be noted that in this case, the $^{19}\text{F} + ^{194}\text{Pt}$ system (^{213}Fr , $N_c = 126$) has a neutron shell closure similar to $^{12}\text{C} + ^{198}\text{Pt}$ system (^{210}Po , $N_c = 126$) reported earlier. If the earlier conjecture is correct, then it is expected that while the $^{19}\text{F} + ^{198}\text{Pt}$ system (^{217}Fr , $N_c = 130$) should exhibit normal anisotropies consistent with SSPM predictions, the system $^{19}\text{F} + ^{194}\text{Pt}$ (^{213}Fr , $N_c = 126$) should display anomalous anisotropies.

II. EXPERIMENTAL DETAILS

The fission data for the above-mentioned systems have been measured using the BARC-TIFR 14 UD Pelletron accelerator at Bombay. The measurements have been carried out in the laboratory energy range from 88 to 104 MeV, using self-supporting rolled foils of ^{194}Pt (97.4% enriched, 1 mg/cm² thick) and ^{198}Pt (95.7% enriched, 1.3 mg/cm² thick). Fission fragment angular distributions were measured from 80° to 170° in laboratory. Two $\Delta E - E$ telescopes consisting of Si surface barrier detectors (thicknesses $\Delta E = 10 - 15 \mu\text{m}$, $E = 300 \mu\text{m}$) were used to detect the fission fragments. The Si telescopes are operated deriving the trigger signal from the ΔE detectors. Most of the fission fragments are stopped in ΔE detector while fragments reaching the E detector were well separated from the direct reaction products and evaporated particles in the two dimensional E vs ΔE plot. Two Si surface barrier detectors, kept at 35° and 55° to monitor Rutherford scattering, were used for absolute normalization of fission cross sections. Measured fission fragment angular distributions were transformed to center of mass using Viola's systematics [5] for symmetric fission. Angular distributions in center of mass $W(\theta)$ were fitted with the standard expression for angular distribution [2,6,7]. Typical angular distributions along with the fits are shown in Fig. 1. Angle integrated fission cross sections and fission fragment angular anisotropies, $A = W(180^\circ)/W(90^\circ)$ obtained from the angular distributions are listed in Tables I and II, respectively. The fission excitation functions are plotted in Fig. 2. As expected, the more fissile compound nuclear system $^{19}\text{F} + ^{194}\text{Pt}$ exhibits significantly larger fission cross section over the entire energy range when compared to that of the less fissile $^{19}\text{F} + ^{198}\text{Pt}$ system. At a few energies ($E \approx 90, 96, \text{ and } 103 \text{ MeV}$) the evaporation residue (ER) cross sections have been measured by off beam γ activity measurement after irradiation using an efficiency calibrated 60-cm³ HPGe detector. As the α decay half-lives of the ERs are small, the γ activity following the electron capture of daughter nuclei (formed from α decay) has been made use of to determine the production cross section of ER. The overall error on ER cross section is estimated to be about 10%,

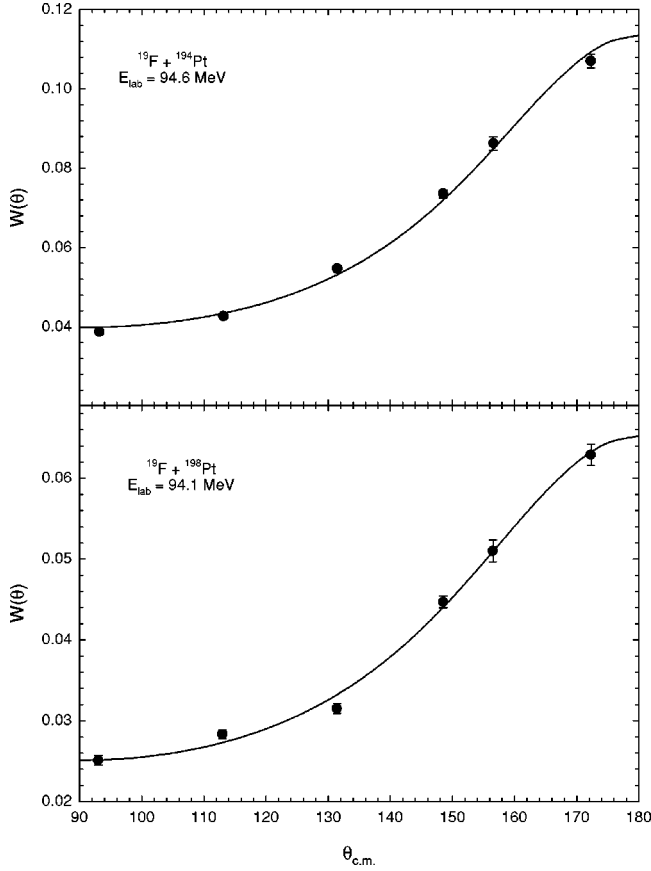


FIG. 1. Fission fragment angular distribution for $^{19}\text{F}+^{194}\text{Pt}$ at $E_{lab}=94.6$ MeV (top panel) and for $^{19}\text{F}+^{198}\text{Pt}$ at $E_{lab}=94.1$ MeV (bottom panel). Continuous lines are the fits using the standard expression discussed in the text.

consisting of uncertainties in γ branching ratio and detector efficiency in addition to counting statistics. At these three energies, where both fission and evaporation residue cross sections are available (Table II), it has been possible to determine the fusion cross sections for both the systems. In Fig. 2, the fission probability P_f values are also plotted (inset).

III. RESULTS AND DISCUSSION

At a given bombarding energy, the fission anisotropy for $^{19}\text{F}+^{194}\text{Pt}$ is expected to be lower than that for $^{19}\text{F}+^{198}\text{Pt}$ for the following reasons: The excitation energy of the compound nucleus formed through $^{19}\text{F}+^{194}\text{Pt}$ channel is about 3 MeV higher than that of the other system. This leads to higher temperature and K_o^2 (variance of K distribution) at the saddle. This will result in lower fission anisotropy value. Also for the more fissile system $^{19}\text{F}+^{194}\text{Pt}$, the second moment of the spin distribution ($\langle l^2 \rangle$) related to fission is expected to be lower than that of the latter system, implying smaller fission anisotropy. However, surprisingly the measured anisotropies of the two systems are similar over the entire energy range.

The measured fusion cross sections have been fitted using the coupled channels code CCFUS [8], in order to determine the spin distribution of the decaying compound nucleus. For

TABLE I. Fission fragment anisotropies for the systems $^{19}\text{F}+^{194,198}\text{Pt}$.

$^{19}\text{F}+^{194}\text{Pt}$		$^{19}\text{F}+^{198}\text{Pt}$	
E_{lab} (MeV)	Anisotropy	E_{lab} (MeV)	Anisotropy
88.6	2.19 ± 0.12	88.1	1.91 ± 0.12
90.6	2.13 ± 0.12	90.1	2.10 ± 0.12
92.6	2.35 ± 0.14	92.1	2.42 ± 0.11
94.6	2.86 ± 0.24	94.1	2.63 ± 0.18
96.6	2.99 ± 0.15	96.1	2.88 ± 0.12
101.6	2.82 ± 0.12	101.1	3.11 ± 0.12
103.6	3.12 ± 0.12	103.1	3.53 ± 0.14

these calculations the low-lying states of both the target and the projectile have been included. As the fusion data are available only at three energies ($E \approx 90, 96,$ and 103 MeV), the l distribution values of the compound nucleus required at the other energies have been obtained from the CCFUS predictions. With the compound nucleus spin distribution fixed by the above prescription, the statistical model calculations have been performed using the code PACE [9] to reproduce the ER cross section σ_{ER} and the fission cross section σ_{fiss} for both the systems. As has been noted in the literature, the three principal parameters that influence the cross sections, the fission probability P_f and the prefission neutron multiplicities ν_{pre} are the angular momentum dependent fission barrier height [$B_f(l)$], the ratio of the level density parameters at the saddle to the equilibrium deformations a_f/a_n and the level density parameter at equilibrium deformation a_n . Besides the measured σ_{fiss} and σ_{ER} , use has been made of the ν_{pre} data available for $^{19}\text{F}+^{198}\text{Pt}$ and $^{16}\text{O}+^{197}\text{Au}$ [10] (populating the same compound nucleus as $^{19}\text{F}+^{194}\text{Pt}$) to constrain the statistical model parameters. For a_n , the energy dependent shell correction from Ref. [11] with the asymptotic value of $A/9$ has been employed. Use of the experimental mass rather than liquid drop mass gave better fits to the data, in particular, the partial ER data. The values of $B_f(l)$ [12], and a_f/a_n have been varied to optimize the fits to the entire data set. Final set of SM parameters used are $B_f = 1.17 \times B_f(\text{Sierk})$, $a_f/a_n = 1.015$ for $^{19}\text{F}+^{194}\text{Pt}$ system and $B_f = 1.17 \times B_f(\text{Sierk})$, $a_f/a_n = 1.050$ for $^{19}\text{F}+^{198}\text{Pt}$ system. The statistical model fits to the σ_{fiss} and the P_f data are shown in Fig. 2.

With the SM parameters fixed as described above, calculations have been made for the fission fragment anisotropies in terms of the SSPM. These calculations essentially depend on the spin distribution of the fissioning nucleus, effective moment of inertia J_{eff} , and the temperature at the saddle point. As pointed out earlier [3], multichance, high spin fission could be very sensitive to shell corrections as fission from the later stages occur from relatively colder nuclei. Fission angular distributions have been calculated using the procedure suggested by Vigdor *et al.* [3] for multichance fission. However, in the present study the exact expression for angular distribution [2] has been used to calculate fission fragment anisotropy values. Excitation energy and spin distributions of fissioning nuclei for each chance fission are taken

TABLE II. Measured fusion and evaporation residue cross sections for $^{19}\text{F}+^{194,198}\text{Pt}$ systems.

$^{19}\text{F}+^{194}\text{Pt}$			$^{19}\text{F}+^{198}\text{Pt}$		
E_{lab} (MeV)	$\sigma_{fission}$ (mb)	σ_{ER} (mb)	E_{lab} (MeV)	$\sigma_{fission}$ (mb)	σ_{ER} (mb)
88.6	35.5 ± 2.5		88.1	19.0 ± 1.5	
90.6	72.8 ± 5.1	42.8 ± 4.0	90.1	41.4 ± 3.0	67.5 ± 7.0
92.6	113 ± 6		92.1	68.3 ± 4.1	
94.6	161 ± 10		94.1	101 ± 6	
96.6	225 ± 13	87.5 ± 9.0	96.1	140 ± 8	158 ± 16
103.6	498 ± 25	42.3 ± 5.0	103.1	335 ± 17	205 ± 20

from PACE predictions. J_{eff} values are taken from Ref. [12].

The measured and the calculated fission anisotropies are compared as a function of bombarding energy for $^{19}\text{F}+^{194}\text{Pt}$ and $^{19}\text{F}+^{198}\text{Pt}$ system in Figs. 3 and 4, respectively. The dashed lines represent the SSPM calculations. It is found that, in general, the calculations overpredict the data. As the various SM parameters have been optimized by demanding fits to σ_{fiss} , σ_{ER} , and ν_{pre} data (wherever available), the parameter J_{eff} , which influences the fission angular distributions, has been multiplied by a suitable factor in order to make the calculated anisotropies agree with the data. The final J_{eff} values are obtained by averaging over the entire energy range. Multiplicative factors to Sierk's J_{eff} values used are 1.21 ± 0.17 for $^{19}\text{F}+^{194}\text{Pt}$ and 1.37 ± 0.15 for $^{19}\text{F}+^{198}\text{Pt}$. The errors in the multiplicative factors represent the standard deviations. It is found that the J_{eff} normalized calculations agree with the anisotropy data in the case of $^{19}\text{F}+^{198}\text{Pt}$ system over the entire energy range except at the highest energy point. However, in the case of $^{19}\text{F}+^{194}\text{Pt}$ system, though the data are on the average in good accord with the calculations, noticeable deviations between the data and the calculations are seen at a few energies. Fission hindrance and the resulting enhanced pre-fission neutron emission, which are significant for $E_X \sim 60$ MeV onwards, have not

been considered in the present SM calculations. So, the disagreement between theory and the experiment at the highest energy in case of $^{19}\text{F}+^{198}\text{Pt}$ system can be understood as arising due to noninclusion of enhanced pre-fission neutron emission as a result of fission dissipation. However, the above discrepancy at $E_X \sim 60$ MeV is not observed in $^{19}\text{F}+^{194}\text{Pt}$ system, which implies reduced dissipation effect compared to the other system. This observation is consistent with the result of Back *et al.* [13], who found the threshold E_X for fission dissipation effect to be significantly higher in case of shell closed nuclei compared to that for nonshell closed nuclei.

It is interesting to compare the present results with that reported in Ref. [1]. It may be mentioned that in SSPM calculations reported earlier [1], the fission fragment angular distribution for each chance was not determined separately. In Ref. [1] the angular momentum distribution of the fissioning nuclei was obtained as $\sigma(l)P_f(l)$, where $\sigma(l)$, is the fusion angular momentum distribution and $P_f(l)$, is the cumulative fission probability (adding all multichance fission contributions) for each l . Further, in calculating the saddle point temperature an average value of presaddle neutron number was assumed. In Fig. 5 the results for $^{12}\text{C}+^{194,198}\text{Pt}$ systems as reported in Ref. [1] are shown

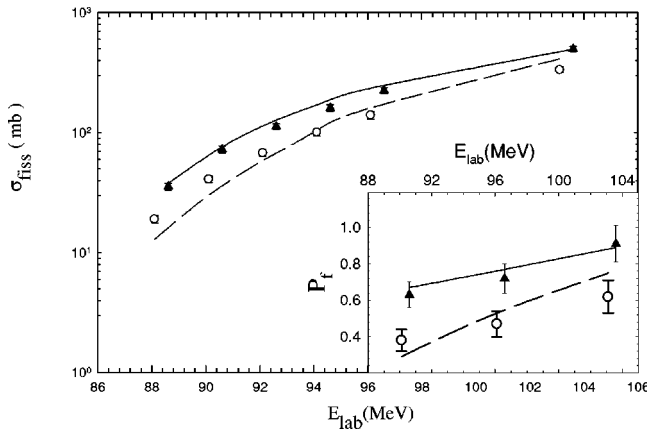


FIG. 2. The measured fission excitation functions for the systems $^{19}\text{F}+^{194,198}\text{Pt}$ (filled triangles for $^{19}\text{F}+^{194}\text{Pt}$ and open circles for $^{19}\text{F}+^{198}\text{Pt}$) and comparison with the statistical model calculations (continuous line for $^{19}\text{F}+^{194}\text{Pt}$ and dashed line for $^{19}\text{F}+^{198}\text{Pt}$). The measured fission probability values are also compared with the statistical model calculations (inset).

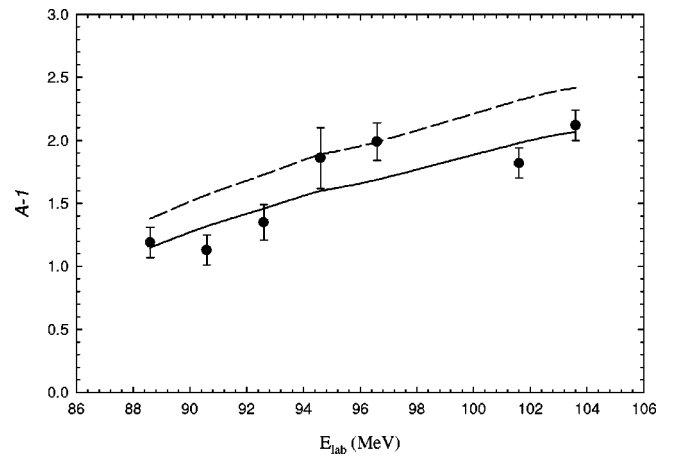


FIG. 3. The fission fragment anisotropy (A) values plotted as a function of bombarding energy for $^{19}\text{F}+^{194}\text{Pt}$ system. The continuous and the dashed lines represent the SSPM calculations made using Sierk's J_{eff} values and normalized Sierk's J_{eff} values, respectively.

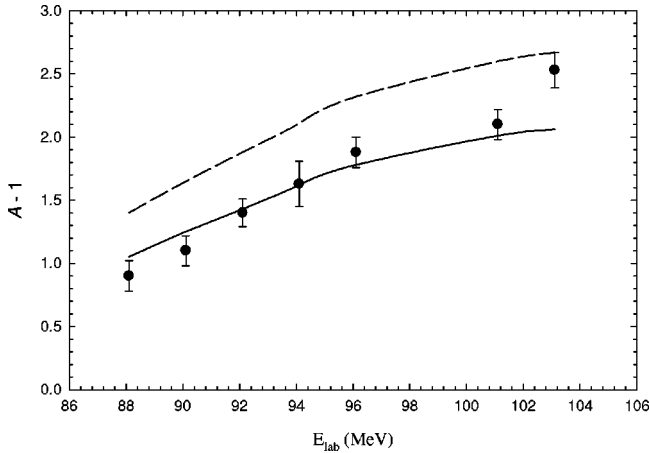


FIG. 4. The fission fragment anisotropy values plotted as a function of bombarding energy $^{19}\text{F} + ^{198}\text{Pt}$ system. The continuous and the dashed lines have the same meaning as in Fig. 3.

as dashed lines. The $^{12}\text{C} + ^{194,198}\text{Pt}$ data have been re-analyzed taking into account explicitly the multichance fission contributions (calculating fission fragment angular distribution for each chance separately) and the results are shown in Fig. 5 as continuous lines. Statistical model parameters used to explain fission and ERs excitation functions are $B_f = 1.05 \times B_f(\text{Sierk})$, $a_f/a_n = 1.006$ and $B_f = 1.07 \times B_f(\text{Sierk})$, $a_f/a_n = 1.000$ for $^{12}\text{C} + ^{194}\text{Pt}$ and $^{12}\text{C} + ^{198}\text{Pt}$ system, respectively. Multiplicative factor to Sierk's J_{eff} are 1.54 ± 0.12 and 0.96 ± 0.10 for $^{12}\text{C} + ^{194}\text{Pt}$ and $^{12}\text{C} + ^{198}\text{Pt}$ system, respectively. It can be seen from Fig. 5 that there is a good agreement between the experiment and the theory for $^{12}\text{C} + ^{194}\text{Pt}$ system over the entire energy range. For $^{12}\text{C} + ^{198}\text{Pt}$, the SSPM calculations are on the average in good accord with the experimental data. However, the lowest energy point is still deviant but much less compared to the earlier result.

IV. SUMMARY

Fission fragment angular anisotropies have been measured and compared with SSPM calculations considering multichance fission decay. Fission anisotropy values calculated using Sierk's J_{eff} values overpredict the data. Hence, normalized Sierk's J_{eff} values have been used in the calculations. Measured anisotropy values can be reproduced by SSPM calculation for $^{19}\text{F} + ^{198}\text{Pt}$ system over the entire energy range. In case of $^{19}\text{F} + ^{194}\text{Pt}$ system, noticeable deviations between data and calculated values have been seen at a

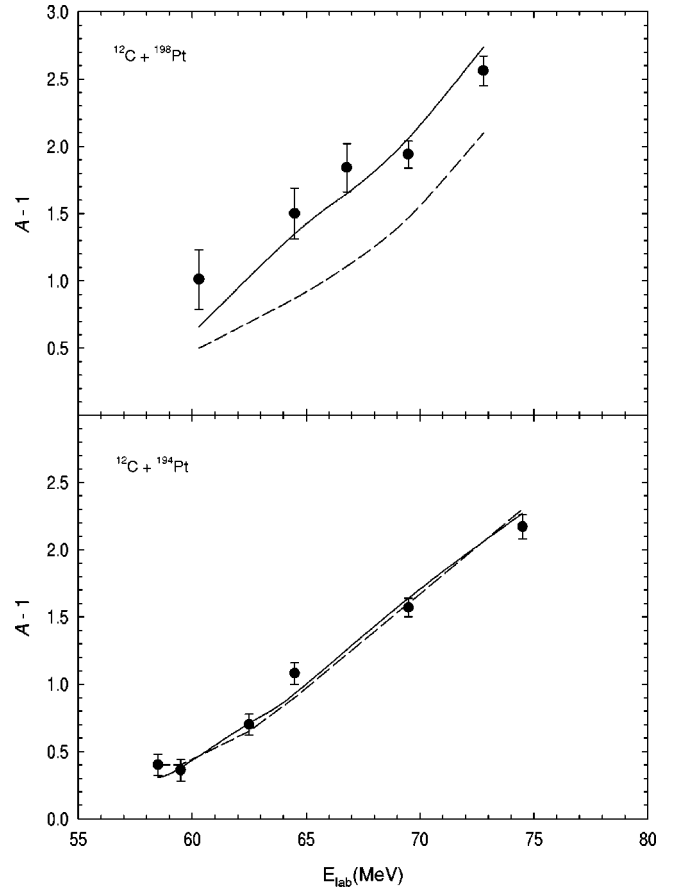


FIG. 5. The fission fragment anisotropy (A) values are plotted as a function of bombarding energy for $^{12}\text{C} + ^{198}\text{Pt}$ (top panel) and $^{12}\text{C} + ^{194}\text{Pt}$ (bottom panel). The dashed lines represent the calculation as reported earlier in Ref. 1. The continuous lines are the new calculation taking into account multichance fission as discussed in the text.

few energies. It has been shown that the deviation between data and SSPM calculations is considerably reduced for $^{12}\text{C} + ^{198}\text{Pt}$ system when multichance fission contribution is properly treated.

ACKNOWLEDGMENTS

The authors thank Dr. S. S. Kapoor for his keen interest in this work and useful suggestions. The authors acknowledge the support of the Pelletron accelerator crew for the excellent beam quality throughout the experiment. Thanks are also due to Dr. A. Navin for his help during the experiment.

- [1] A. Shrivastava, S. Kailas, A. Chatterjee, A.M. Samant, A. Navin, P. Singh, and B.S. Tomar, Phys. Rev. Lett. **82**, 699 (1999).
- [2] R. Vandenbosch and J. R. Huizenga, *Nuclear Fission* (Academic Press, New York, 1973).
- [3] S.E. Vigdor, H.J. Karwowski, W.W. Jacobs, S. Kailas, P.P. Singh, F. Soga, and P. Yip, Phys. Lett. **90B**, 384 (1980).
- [4] B. Djerroud *et al.*, Phys. Rev. C **61**, 024607 (2000).

- [5] V.E. Viola, K. Kwiatkowski, and M.E. Walker, Phys. Rev. C **31**, 1550 (1985).
- [6] I. Halpern and V.M. Strutinsky, *Proceeding of International Conference on Peaceful uses of Atomic Energy, Geneva* (United Nations, Geneva, 1958), Vol. 15, p. 408.
- [7] B.B. Back, R.R. Betts, J.E. Gindler, B.D. Wilkins, S. Saini, M.B. Tsang, C.K. Gelbke, W.G. Lynch, M.A. McMahan, and P.A. Baisden, Phys. Rev. C **32**, 195 (1985).

- [8] C.H. Dasso and S. Landowne, *Comput. Phys. Commun.* **46**, 187 (1987).
- [9] A. Gavron, *Phys. Rev. C* **21**, 230 (1980).
- [10] D.J. Hinde, D. Hilscher and H. Rossner, *Nucl. Phys.* **A502**, 497c (1989); J.O. Newton, *Pramana J. Phys.* **33**, 175 (1989).
- [11] A.V. Ignatyuk, G.N. Smirenkin, and A.S. Tishin, *Sov. J. Nucl. Phys.* **21**, 255 (1975).
- [12] A.J. Sierk, *Phys. Rev. C* **33**, 2039 (1986).
- [13] B.B. Back, D.J. Blumenthal, C.N. Davids, D.J. Henderson, R. Hermann, D.J. Hofman, C.L. Jiang, H.T. Penttila, and A.H. Wuosmaa, *Phys. Rev. C* **60**, 044602 (1999).